ORIGINAL ARTICLE

In vivo detection of beta-amyloid at the nasal cavity and other skull-base sites: a retrospective evaluation of ADNI1/GO

Anish Kapadia[1,2] · Prarthana Desai[3] · Adam Dmytriw[1,2] · Pejman Maralani[1,2] · Chris Heyn[1,2] · Sandra Black[4,5] · Sean Symons[1,2] · For the Alzheimer's Disease Neuroimaging Initiative

Abstract

Introduction Amyloid beta (Aβ) is partially cleared from the CSF via skull base perivascular and perineural lymphatic pathways, particularly at the nasal cavity. In vivo differences in Aβ level at the nasal cavity between patients with Alzheimer's disease (AD), subjects with mild cognitive impairment (MCI) and cognitively normal (CN) individuals have not been previously assessed.

Methods This is a retrospective evaluation of subject level data from the ADNI-1/GO database. Standardized uptake value ratio (SUVR) maximum on ^{11}C-Pittsburgh compound-B (PiB)-PET was assessed at the nasal cavity on 223 scans. Exploratory ROI analysis was also performed at other skull base sites. SUVR maximum values and their differences between groups (CN, MCI, AD) were assessed. CSF Aβ levels and CSF Aβ 42/40 ratios were correlated with SUVR maximum values.

Results 103 subjects with 223 PiB-PET scans (47 CN, 32 AD and 144 MCI) were included in the study. The SUVR maxima at the nasal cavity were significantly lower in subjects with AD [1.35 ($\pm$0.31)] compared to CN [1.54 ($\pm$0.30); p = 0.024] and MCI [1.49 ($\pm$0.33); p = 0.049]. At very low CSF Aβ, less than 132 pg/ml, there was significant correlation with nasal cavity SUVR maximum. The summed averaged SUVR maximum values were significantly lower in subjects with AD [1.35 ($\pm$0.16)] compared to CN [1.49 ($\pm$0.17); p = 0.003] and MCI [1.40 ($\pm$0.17); p = 0.017].

Conclusion Patients with AD demonstrate reduced nasal cavity PiB-PET radiotracer uptake compared to MCI and CN, possibly representing reduced Aβ clearance via perineural/perivascular lymphatic pathway. Further work is necessary to elucidate the true nature of this finding.

Keywords Neurology · Pathogenesis · Alzheimer's Amyloid

Background

Alzheimer's disease (AD) is one of the leading causes of dementia, only second to mixed dementia in terms of prevalence [1, 2]. The overall social and economic burden is well recognized, with direct healthcare cost and economic impact

✉ Anish Kapadia
anish.kapadia@mail.utoronto.ca

Extended author information available on the last page of the article

on caregivers approaching an estimated half a trillion dollars in the US [3]. The number of individuals diagnosed with AD is projected to increase, particularly in developed countries with aging populations. This underlines the increasing urgency for the development of disease-modifying therapies, and the 2013 G8 Dementia Summit targeted 2025 for the development of a cure [4]. Understanding the pathophysiology is essential in the development of a successful intervention. Extracellular amyloid beta (Aβ) plaque deposition, intracellular neurofibrillary tangles (NFTs) of phosphorylated tau and neuronal loss are the histologic hallmarks of AD [5]. The pathologic process precedes the clinical stage of disease by many years, with deposition of Aβ and tau serving as early biomarkers [6]. One of the leading hypotheses for AD pathophysiology is the amyloid hypothesis which postulates that the disease develops over time due to an imbalance in Aβ production and clearance. Current evidence

suggests that patients with sporadic AD have impaired Aβ clearance, rather than dysregulated production [7]. The clearance of Aβ from the CNS is thought to be multifaceted with evidence for degradation or microglial phagocytosis within the CNS, clearance through the blood–brain barrier (BBB) into the systemic circulation, and more recently clearance via the meningeal lymphatics [8]. CSF clearance via perineural pathways, specifically via the nasal lymphatics through the cribriform plate has been shown in multiple animal and human studies [9],[10], and solutes in the CSF may be cleared via this pathway [11]. There is evidence for Aβ clearance to cervical and axillary lymph nodes in mice, posited to be via this lymphatic mechanism [12]. Positron emission tomography (PET) imaging in human subjects has demonstrated an inverse relationship between dynamic CSF clearance to the nasal cavity and brain Aβ levels [13]. Currently, there are no in vivo studies in humans identifying Aβ at the level of the nasal cavity [13]. Amyloid PET imaging allows for in vivo assessment of Aβ deposition. ^{11}C-Pittsburgh compound-B (PiB)—PET has been extensively studied and demonstrates strong agreement with histologic Aβ deposition [14].

The primary objective of this study was to assess PiB radiotracer uptake along the posited nasal (and skull base) lymphatic CSF clearance pathway, and determine whether there is an association between radiotracer uptake and diagnosis of AD dementia [15], Mild Cognitive Impairment [16] and normal aging. We hypothesised that PiB radiotracer uptake would be identified within the nasal cavity in all subjects, and reduced uptake would be seen in patients with AD.

METHODS

Subjects

Data used in the preparation of this article were obtained from the Alzheimer's disease Neuroimaging Initiative (ADNI) database (http://adni.loni.usc.edu). The ADNI was launched in 2003 as a public–private partnership, led by Principal Investigator Michael W. Weiner, MD. The primary goal of ADNI has been to test whether serial magnetic resonance imaging (MRI), positron emission tomography (PET), other biological markers, and clinical and neuropsychological assessment can be combined to measure the progression of mild cognitive impairment (MCI) and early Alzheimer's disease (AD) [17]. Institutional Review Board approval was obtained at each site. Written informed consent was obtained from all subjects, or their authorized representatives.

Subject level data from the ADNI phases 1/GO (ADNI-1/GO) from patients who underwent PIB PET with post-processing for quantification were obtained. The post-processed PIB PET images were assessed for quality control with the intent of excluding those with significant artifact or lack of coverage of the areas of concern. Data for CSF biomarkers, namely amyloid-β (Aβ1–42), total tau (t-tau) and phosphorylated tau (p-tau181), corresponding to those with post-processed PIB PET scans were downloaded December 21, 2019. Subjects were stratified using the current clinical diagnosis as defined by ADNI: (1) clinically normal (CN) (2) mild cognitive impairment (MCI) and (3) dementia due to AD.

PiB-PET acquisition, post-processing and analysis

PiB PET scan acquisition and post-processing for ADNI have been previously summarized in detail [18],[19]. Briefly, PiB-PET acquisition was completed on multiple PET scanners and with multiple acquisition sequences. In general, the acquisition protocol was injection of approximately 10–15 mCi of [^{11}C]PiB with an uptake period of approximately 50 min. Acquisition was performed at a rate of 4–5 min frames. Quality control (QC) was performed on all scans. The raw data underwent post-processing to allow quantification, which involved (1) aligning the frame and averaging to create a single image, (2) standardization of orientation and voxel size, (3) intensity normalization using the cerebellar grey matter, and (4) smoothing to a common resolution. The post-processed images, "PIB Coreg, Avg, Std Img and Vox Size, Uniform Resolution", available from the LONI ADNI site (http://adni.loni.ucla.edu/) were downloaded for this study. The accompanying data on SUVR analysis of various brain areas were also downloaded [20].

Post-processed images were evaluated on a DICOM viewer with multi-planar reformat capabilities. Images were analyzed by a board-certified radiologist (AK). Region of interest (ROI) analysis was performed to quantify the maximal SUVR at the nasal cavity (Fig. 1), clivus, bilateral jugular foramen, bilateral masticator space and calvarial vault. Individual scans underwent further QC for signal noise and artifact; the inferior most slices of each scan were excluded due to signal noise. The jugular foramen and masticator space ROIs were most commonly excluded due to lack of coverage or noise, resulting from the more caudal anatomic position. It should be noted that these sites were not the primary focus of the analysis. In addition, brain amyloid plaque load (BAPL) score was assigned for each scan with scores of 1, 2 and 3 indicating no Aβ load, minor Aβ load and significant Aβ load [21].

CSF biologic marker

Data for CSF biomarkers amyloid-β (Aβ1–42) were extracted from the "UPENNBIOMK_MASTER.csv" which was downloaded from the LONI ADNI site on December 21, 2019 (http://adni.loni.ucla.edu/). Biomarker values for

Fig. 1 PIB-PET images with multi-planar reformats (**a**—coronal, **b**—axial, **c**—sagittal) demonstrating radiotracer uptake in the anterior nasal cavity, in the region of the olfactory recess (arrow). ROI analysis was performed on axial images as demonstrated in **b** (red oval) with maximum SUVR noted
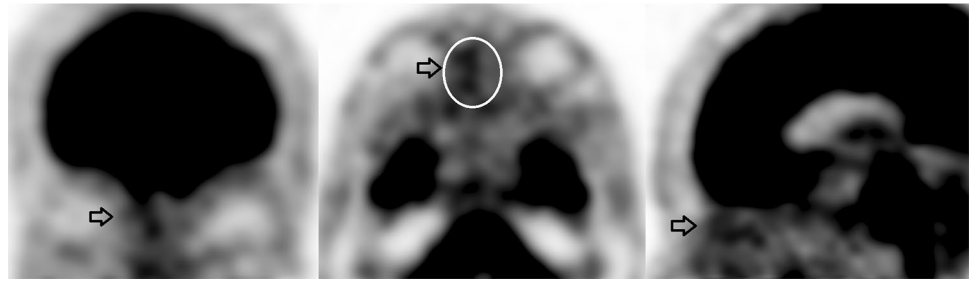
sample draw dates corresponding to the PiB PET scan were included, within 3 months of the scan date, as previously validated [22–24].

Statistical analysis

The group-wise differences in the PiB PET SUVR at the nasal cavity, clivus, bilateral jugular foramina and bilateral masticator space were assessed using ANOVA. Association between SUVR data and CSF Aβ1–42 assessment was performed using linear regression. Additional group-wise analysis for association was also performed using linear regression. Mixed-effect analysis was performed to further analyze the association between SUVR data and CSF Aβ1–42. Thresholding of CSF Aβ1–42 was performed at 192 pg/ml, a sensitive marker for differentiating AD from CN individuals [25], and of very low values below 132 pg/ml, a median value in AD patients [26]. Statistical significance was set at a p value of < 0.05. Analysis was performed using R (R 64X 3.4.4).

Data availability

Data used for the present study will be made available to other investigators upon reasonable request. The raw data for this study are also available on the ADNI database (http://adni.loni.ucla.edu/).

Results

103 subjects (33% female) with 223 PiB-PET scans (47 CN, 32 AD and 144 MCI) were included in the study. The average age at scan was 73.7 ($\pm$ 9.0), 78.9 ($\pm$ 5.3) and 75.9 ($\pm$ 7.9) for AD, CN and MCI, respectively. Distributions of BAPL scores for the sample for grade 1, grade 2 and grade 3 were 21.5%, 15.7% and 62.8%, respectively. The proportion of BAPL grade 3 scans was significantly higher in the AD group (p = 0.006). CSF analysis was available for a subgroup of 82 scans within 3 months of the PiB-PET scan, with 12 AD, 16 CN and 53 MCI scans. The SUVR maximum values at the nasal cavity were 1.35 ($\pm$ 0.31), 1.54 ($\pm$ 0.30) and 1.49 ($\pm$ 0.33) for AD, CN and MCI subjects, respectively. The nasal cavity SUVR maximum was significantly lower in subjects with AD compared to CN individuals (p = 0.024) and those with MCI (p = 0.049) on pairwise analysis (Fig. 2). There were no differences in nasal cavity SUVR based on BAPL score (p = 0.80). The CSF Aβ levels were 122.65 ($\pm$ 18.23), 172.88 ($\pm$ 49.39) and 158.67 ($\pm$ 50.62) for AD, CN and MCI subjects, respectively (Fig. 3). The CSF Aβ was significantly lower in subjects with AD compared to CN individuals (p = 0.016) and those with MCI (p = 0.046) on pairwise analysis. CSF Aβ was significantly lower in subjects with AD compared to CN individuals (p $\ll$ 0.001) and those with MCI (p $\ll$ 0.001) on pairwise analysis. The ratios of CSF Aβ 42/40 were 0.078 ($\pm$ 0.023), 0.114 ($\pm$ 0.042) and 0.095 ($\pm$ 0.031) for AD, CN and MCI subjects (respectively).

Fig. 2 Plot of mean SUVR with standard error by subject subgroup for nasal cavity SUVR maximum and averaged skull base SUVR maximum. *·**Significant difference with $p < 0.05$ on pairwise ANOVA analysis. *AD* Alzheimer's disease, *MCI* mild cognitive impairment, *CN* cognitively normal
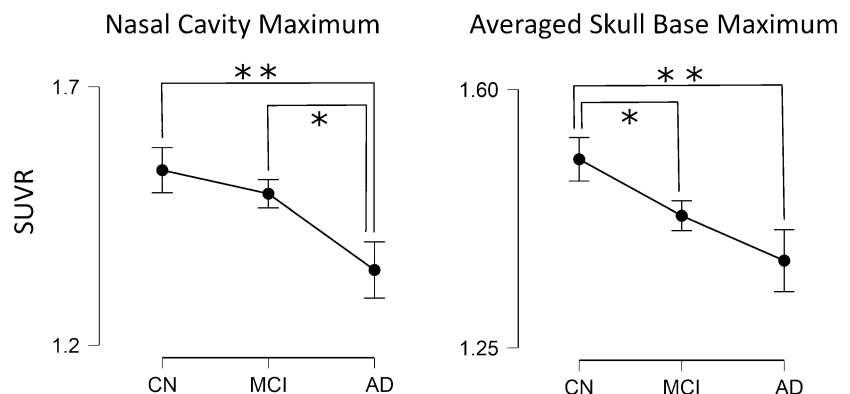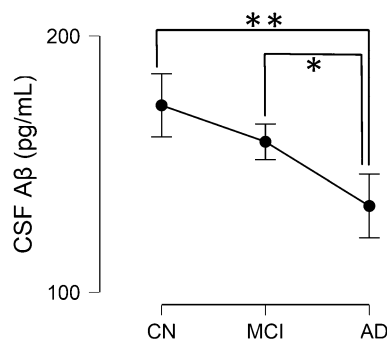
Fig. 3 Plot of mean CSF Aβ concentration by subgroup. *,**Significant difference with p < 0.05 on pairwise ANOVA analysis. *AD* Alzheimer's disease, *MCI* mild cognitive impairment, *CN* cognitively normal

The ratio of CSF Aβ 42/40 was significantly lower in AD compared to CN individuals (p = 0.033). No significant correlation was seen between nasal cavity SUVR maximum, and CSF Aβ or the ratio of CSF Aβ 42/40 for the sample. In addition, at CSF Aβ less than 192 pg/ml or less, there was no correlation with SUVR maximum. However, at very low CSF Aβ levels, less than 132 pg/ml, there was a positive correlation with SUVR maximum (R-squared 0.14, p = 0.028). No significant correlation was seen between nasal cavity SUVR maximum and CSF Aβ within groups for diagnosis or BAPL grade.

In addition, exploratory assessment was performed at the jugular foramina, upper masticator spaces and clivus (Supplemental Table and Figs. 1–3). The summed average of the SUVR maximum at all skull base site was assessed. The summed averaged SUVR maximum values across the skullbase were 1.35 (± 0.16), 1.49 (± 0.17) and 1.40 (± 0.17)

for AD, CN and MCI subjects, respectively. Values were significantly lower in subjects with AD compared to CN individuals (p = 0.003) and those with MCI (p = 0.017). Calvarial vault ROI analysis revealed SUVR maximum of 0.74 (± 0.18), 0.82 (± 0.22) and 0.76 (± 0.17) for AD, CN and MCI subjects, respectively. No significant differences were seen between the groups (Table 1).

The available data on brain SUVR values were used to assess group-wise differences. No significant association was observed between nasal SUVR maximum and regional brain SUVR values. Significant group-wise differences in SUVR were seen at pertinent areas including the parietal cortex and precuneus with higher values seen in AD in these areas (Supplemental Fig. 1). Regression analysis of these areas demonstrates strong and very significant association with CSF Aβ (Supplemental Table 2).

Discussion

We demonstrate that PiB radiotracer uptake can be observed within the nasal cavity and, more generally, can be seen at the skull base. Individuals with AD demonstrate significantly less radiotracer activity at the nasal cavity and skull base compared to those with MCI and CN, a trend which is paralleled by the CSF Aβ level. A correlation between the radiotracer activity and CSF Aβ or CSF Aβ 42/40 ratio could not be established for the whole sample. However, significant positive correlation between CSF Aβ and radiotracer activity was seen at CSF Aβ levels below 132 pg/ml (Fig. 4).

The underpinning physiology for PiB radiotracer uptake at these skull base sites remains unclear, and there are several considerations. First, PiB may be actively cleared from

Table 1 Summary of results of ROI SUVR analysis at the nasal cavity, and summary of CSF Aβ levels by subgroup

	Total	CN	MCI	AD	*p* value
N	223	47	144	32	N/A
Gender (% female)	33.2	42.6	29.9	34.4	N/A
Age (years)	76.2 (± 7.7)	78.9 (± 5.3)	75.9 (± 7.9)	73.7 (± 9.0)	0.012* (ANOVA)
BAPL score (1, 2 and 3)	21.5%, 15.7% and 62.8%	25.5%, 23.4% and 51.1%	24.6%, 15.4% and 61.2%	3.1%, 6.2% and 90.7%	0.006* (Chi-squared)
Nasal cavity SUVR Maximum	1.48(± 0.32)	1.53 (± 0.30)	1.49 (± 0.33)	1.35 (± 0.31)	0.025* (ANOVA)
Nasal cavity SUVR Average	1.08(± 0.25)	1.17 (± 0.23)	1.07 (± 0.25)	1.00 (± 0.23)	0.011* (ANOVA)
Calvarial vault SUVR Maximum	0.78 (± 0.19)	0.82 (± 0.22)	0.76 (± 0.17)	0.74 (± 0.18)	NS (ANOVA)
N	82	16	53	12	N/A
CSF Aβ level (pg/ml)	1.57.47(± 50.32)	172.88 (± 49.39)	158.67 (± 50.62)	122.65 (± 18.23)	0.019* (ANOVA)
CSF Aβ 42 / 40 ratio	0.096 (± 0.034)	0.114 (± 0.042)	0.095 (± 0.031)	0.078 (± 0.023)	0.042* (ANOVA)

AD Alzheimer's disease, *MCI* mild cognitive impairment, *CN* cognitively normal

*Significant difference with *p* < 0.05 on pairwise ANOVA analysis
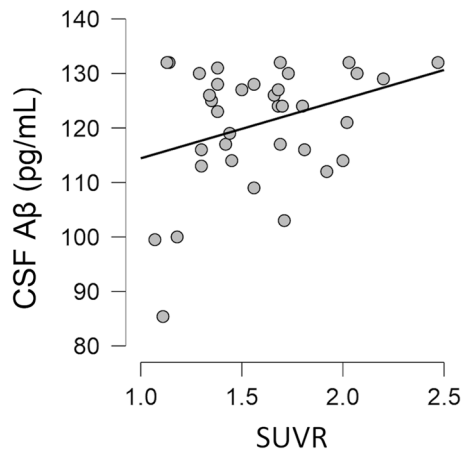
Fig. 4 Scatter plot of CSF Aβ concentration and maximum nasal cavity SUVR with least square line for subjects with very low CSF Aβ concentration equal to or less than 132 pg/mL

the CSF via the skull base lymphatics, either bound to Aβ or independently. The possibility of these findings representing dynamic clearance of CSF Aβ is particularly intriguing; if correct, this would allow for the development of a novel imaging biomarker of CSF Aβ clearance to the lymphatic system. There is prior evidence of an inverse relationship between CSF Aβ levels and rate of dynamic CSF clearance [13]. As such, nasal cavity PiB uptake would be expected to relate to the CSF Aβ level; however, this is not observed. A saturation phenomenon may aid to explain this discrepancy; suggested by a correlation between nasal cavity PiB uptake and very low CSF levels, below 132 pg/ml. Alternatively, PiB may be crossing the nasal cavity radiotracer activity may be unrelated to dynamic clearance of CSF Aβ altogether, possibly related to chronic deposition, reflecting a long-term average [27], or secondary to vascular contamination [28]. Alternatively, reduced nasal cavity activity seen in AD may be related to reduced overall availability of the radiotracer due to more robust uptake intra-cranially. Finally, the radiotracer activity may reflect a complex interaction between several different processes.

PiB, a derivative of Aβ binding dye Thioflavin-T, binds Aβ with high affinity. There is strong evidence from pathologic and imaging/pathologic correlative studies supporting specificity of PiB localization, both in animal models and humans [29]–[32]. As such PiB is thought to be a reliable surrogate marker for Aβ [14]. Pathologic studies in multiple animal species and human cadaveric specimens have demonstrated CSF clearance through the nasal lymphatics [14]. There is also evidence of clearance of CNS solutes via this lymphatic pathway, with evidence for Aβ clearance to cervical and axillary lymph nodes seen in mice [11, 12]. Aβ has been shown to reach the nasal cavity in rats via a non-hematogenous route [33]. In transgenic mice model of Alzheimer's disease,

Aβ deposition was seen in the nasal cavity, positively correlated with Aβ deposition in the brain [34]. Aβ42 and tau have been detected in the nasal cavity of humans using in vitro assays using swab samples. However, no differences in the Aβ42 were found between individuals with AD and controls [35]. A more recent study using microelectrode micro-sensor technique has found that nasal cavity Aβ may be elevated in AD [36]. Dynamic PET imaging has demonstrated an inverse relationship between nasal cavity CSF clearance and brain Aβ, as detected by PiB-PET [13]. The authors did identify PiB radiotracer uptake at the nasal cavity; however, no attempts were made to delineate pathologic changes [13]. This is the first in vivo study demonstrating reduced nasal Aβ levels, as reflected by PiB uptake, compared to CN individuals.

The bulk flow of CSF though the brain parenchyma is thought to help clear solutes from the interstitial fluid via a perivascular route [37, 38]. This is felt to be the main mechanism of clearance of ISF Aβ to the CSF [38]. The CSF and solutes can flow out of the CNS via the BBB into the blood stream or along a perineural or perivascular lymphatic route through the skull base. The lymphatic route, via the cervical lymphatics, drains downstream into the blood. In the present study, brain deposition of Aβ is strongly and negatively correlated with CSF Aβ and CSF Aβ 42/40 ratio, known robust marker for amyloid-PET status [39]. The reduced levels of radiotracer uptake at the nasal cavity seen in patients with AD may reflect reduced CSF Aβ clearance, or intrinsically low CSF Aβ levels in this group. We favour the later, given clear prior evidence of reduced CSF Aβ levels and CSF Aβ 42/40 ratio in the AD population [39, 40]. With these current findings in the context of prior literature, we postulate that the failure of clearance of Aβ from the ISF results in interstitial and parenchymal accumulation, and reduced CSF Aβ levels and downstream lymphatic Aβ levels in patients with Alzheimer's disease.

We provide cautious interpretation of the study data, which is limited to retrospective evaluation of available data. There was limited coverage of the skull base on certain individual PiB-PET scans, although the nasal cavity was consistently covered. CSF Aβ levels which were available were often days to months prior to or following the scan, limiting interpretation of its correspondence with the PiB-PET scan analysis in the short term; however, there is previous validation for stability in CSF Aβ [24]. The results of this study are primarily associations and further work is needed to demonstrate causality.

Conclusion

This is the first study to demonstrate in vivo differences in nasal cavity PiB uptake, with reduced levels seen in AD patients. The nasal cavity and skull base PiB uptake may

reflect the clearance of Aβ via the purported skull base lymphatics. Future work is needed to demonstrate precise pathophysiologic mechanism which underpin these findings, with the potential of developing a novel imaging biomarker. A number of questions arise as a result of this study with regard to the mechanism by which Aβ clearance in impeded in Alzheimer's disease.

Compliance with ethical standards

References

1. Barnes DE, Yaffe K. The projected effect of risk factor reduction on Alzheimer's disease prevalence. Lancet Neurol. 2011;10(9):819–28. https://doi.org/10.1016/S1474-4422(11)70072-2.
2. Kapasi A, DeCarli C, Schneider JA. Impact of multiple pathologies on the threshold for clinically overt dementia. Acta Neuropathol. 2017;134(2):171–86. https://doi.org/10.1007/s00401-017-1717-7.
3. Kirson NY, Desai U, Ristovska L, et al. Assessing the economic burden of Alzheimer's disease patients first diagnosed by specialists. BMC Geriatr. 2016. https://doi.org/10.1186/s12877-016-0303-5.
4. G8 Dementia Summit Declaration 2013. Accessed January 11, 2020. http://www.g8.utoronto.ca/healthG8/2013-dementia-declaration.html.
5. Sengoku R. Aging and Alzheimer's disease pathology. Neuropathology. 2020. https://doi.org/10.1111/neup.12626.
6. Tan C-C, Yu J-T, Tan L. Biomarkers for preclinical Alzheimer's disease. J Alzheimer's Dis. 2014;42(4):1051–69. https://doi.org/10.3233/JAD-140843.
7. Mawuenyega KG, Sigurdson W, Ovod V, et al. Decreased clearance of CNS β-amyloid in Alzheimer's disease. Science. 2010;330(6012):1774–1774. https://doi.org/10.1126/science.1197623.
8. Xin S-H, Tan L, Cao X, Yu J-T, Tan L. Clearance of amyloid beta and tau in Alzheimer's disease: from mechanisms to therapy. Neurotox Res. 2018;34(3):733–48. https://doi.org/10.1007/s12640-018-9895-1.
9. Johnston M, Zakharov A, Papaiconomou C, Salmasi G, Armstrong D. Evidence of connections between cerebrospinal fluid and nasal lymphatic vessels in humans, non-human primates and other mammalian species. Fluids Barriers CNS. 2004;1(1):1–13. https://doi.org/10.1186/1743-8454-1-2.
10. Johnston M. The importance of lymphatics in cerebrospinal fluid transport. Lymphat Res Biol. 2003;1(1):41–5. https://doi.org/10.1089/15396850360495682.
11. Louveau A, Smirnov I, Keyes TJ, et al. Structural and functional features of central nervous system lymphatic vessels. Nature. 2015;523(7560):337–41. https://doi.org/10.1038/nature14432.
12. Pappolla M, Sambamurti K, Vidal R, Pacheco-Quinto J, Poeggeler B, Matsubara E. Evidence for lymphatic Aβ clearance in Alzheimer's transgenic mice. Neurobiol Dis. 2014;71:215–9. https://doi.org/10.1016/j.nbd.2014.07.012.
13. de Leon MJ, Li Y, Okamura N, et al. Cerebrospinal fluid clearance in Alzheimer disease measured with dynamic PET. J Nucl Med. 2017;58(9):1471–6. https://doi.org/10.2967/jnumed.116.187211.
14. Driscoll I, Troncoso JC, Rudow GL, et al. Correspondence between in vivo 11C-PiB-PET amyloid imaging and postmortem, region-matched assessment of plaques. Acta Neuropathol. 2012;124:823–31. https://doi.org/10.1007/s00401-012-1025-1.
15. McKhann G, Drachman D, Folstein M, Katzman R, Price D, Stadlan EM. Clinical diagnosis of Alzheimer's disease: report of the NINCDS-ADRDA Work Group under the auspices of Department of Health and Human Services Task Force on Alzheimer's Disease. Neurology. 1984;34(7):939–44. https://doi.org/10.1212/wnl.34.7.939.
16. Petersen RC, Doody R, Kurz A, et al. Current concepts in mild cognitive impairment. Arch Neurol. 2001;58(12):1985–92. https://doi.org/10.1001/archneur.58.12.1985.
17. Weiner MW, Aisen PS, Jack CR, et al. The Alzheimer's disease neuroimaging initiative: progress report and future plans. Alzheimer's Dementia. 2010;6(3):202-211.e7. https://doi.org/10.1016/j.jalz.2010.03.007.
18. Jagust WJ, Landau SM, Shaw LM, et al. Relationships between biomarkers in aging and dementia. Neurology.

2009;73(15):1193–9. https://doi.org/10.1212/WNL.0b013e3181 bc010c.

19. Jagust WJ, Bandy D, Chen K, et al. The Alzheimer's disease neuroimaging initiative positron emission tomography core. Alzheimer's Dementia. 2010;6(3):221–9. https://doi.org/10.1016/j.jalz.2010.03.003.

20. Swaminathan S, Shen L, Risacher SL, et al. Amyloid pathway-based candidate gene analysis of [11C]PiB-PET in the Alzheimer's Disease Neuroimaging Initiative (ADNI) cohort. Brain Imaging Behav. 2012;6(1):1–15. https://doi.org/10.1007/s11682-011-9136-1.

21. Barthel H, Gertz H-J, Dresel S, et al. Cerebral amyloid-β PET with florbetaben (18F) in patients with Alzheimer's disease and healthy controls: a multicentre phase 2 diagnostic study. Lancet Neurol. 2011;10(5):424–35. https://doi.org/10.1016/S1474-4422(11)70077-1.

22. Schindler S, Gray J, Gordon B, et al. Cerebrospinal fluid biomarkers measured by Elecsys assays compared to amyloid imaging. Alzheimer's Dementia. 2018. https://doi.org/10.1016/j.jalz.2018.01.013.

23. Fagan A, Xiong C, Jasielec M, et al. Longitudinal change in CSF biomarkers in Autosomal-dominant Alzheimer's disease. Sci Transl Med. 2014;6:226ra30. https://doi.org/10.1126/scitranslmed.3007901.

24. Blennow K, Zetterberg H, Minthon L, et al. Longitudinal stability of CSF biomarkers in Alzheimer's disease. Neurosci Lett. 2007;419(1):18–22. https://doi.org/10.1016/j.neulet.2007.03.064.

25. Shaw LM, Vanderstichele H, Knapik-Czajka M, et al. Cerebrospinal fluid biomarker signature in Alzheimer's disease neuroimaging initiative subjects. Ann Neurol. 2009;65(4):403–13. https://doi.org/10.1002/ana.21610.

26. Sala A, Nordberg A, Rodriguez-Vieitez E. Longitudinal pathways of cerebrospinal fluid and positron emission tomography biomarkers of amyloid-β positivity. Mol Psychiatry. 2020. https://doi.org/10.1038/s41380-020-00950-w.

27. Kovács T, Cairns NJ, Lantos PL. β-amyloid deposition and neurofibrillary tangle formation in the olfactory bulb in ageing and Alzheimer's disease. Neuropathol Appl Neurobiol. 1999;25(6):481–91. https://doi.org/10.1046/j.1365-2990.1999.00208.x.

28. Tsutsumi S, Ono H, Ishii H, Yasumoto Y. An undescribed venous pathway intervening between the olfactory fossa and nasal vestibule. Surg Radiol Anat. 2019;41(5):485–90. https://doi.org/10.1007/s00276-019-02208-9.

29. Klunk WE, Wang Y, Huang GF, Debnath ML, Holt DP, Mathis CA. Uncharged thioflavin-T derivatives bind to amyloid-beta protein with high affinity and readily enter the brain. Life Sci. 2001;69(13):1471–84. https://doi.org/10.1016/s0024-3205(01)01232-2.

30. Klunk WE, Lopresti BJ, Ikonomovic MD, et al. Binding of the positron emission tomography tracer pittsburgh compound-B

31. Reflects the Amount of amyloid-β in Alzheimer's disease brain but not in transgenic mouse brain. J Neurosci. 2005;25(46):10598–606. https://doi.org/10.1523/JNEUROSCI.2990-05.2005.

31. Mathis CA, Bacskai BJ, Kajdasz ST, et al. A lipophilic thioflavin-T derivative for positron emission tomography (PET) imaging of amyloid in brain. Bioorg Med Chem Lett. 2002;12(3):295–8. https://doi.org/10.1016/s0960-894x(01)00734-x.

32. Fodero-Tavoletti MT, Smith DP, McLean CA, et al. In vitro characterization of Pittsburgh compound-B binding to lewy bodies. J Neurosci. 2007;27(39):10365–71. https://doi.org/10.1523/JNEUROSCI.0630-07.2007.

33. Kameshima N, Yanagisawa D, Tooyama I. β-Amyloid peptide (1–40) in the brain reaches the nasal cavity via a non-blood pathway. Neurosci Res. 2013;76(3):169–72. https://doi.org/10.1016/j.neures.2013.03.016.

34. Kameshima N, Nanjou T, Fukuhara T, Yanagisawa D, Tooyama I. Correlation of Aβ deposition in the nasal cavity with the formation of senile plaques in the brain of a transgenic mouse model of Alzheimer's disease. Neurosci Lett. 2012;513(2):166–9. https://doi.org/10.1016/j.neulet.2012.02.026.

35. Liu Z, Kameshima N, Nanjo T, et al. Development of a high-sensitivity method for the measurement of human nasal Aβ42, tau, and phosphorylated tau. J Alzheimers Dis. 2018;62(2):737–44. https://doi.org/10.3233/JAD-170962.

36. Kim YH, Lee S-M, Cho S, et al. Amyloid beta in nasal secretions may be a potential biomarker of Alzheimer's disease. Sci Rep. 2019;9(1):1–9. https://doi.org/10.1038/s41598-019-41429-1.

37. Abbott NJ. Evidence for bulk flow of brain interstitial fluid: significance for physiology and pathology. Neurochem Int. 2004;45(4):545–52. https://doi.org/10.1016/j.neuint.2003.11.006.

38. Iliff JJ, Wang M, Liao Y, et al. A Paravascular pathway facilitates CSF flow through the brain parenchyma and the clearance of interstitial solutes, including amyloid β. Sci Transl Med. 2012;4(147):147ra111-147ra111. https://doi.org/10.1126/scitranslmed.3003748.

39. Doecke JD, Pérez-Grijalba V, Fandos N, et al. Total Aβ42/Aβ40 ratio in plasma predicts amyloid-PET status, independent of clinical AD diagnosis. Neurology. 2020;94(15):e1580–91. https://doi.org/10.1212/WNL.0000000000009240.

40. Andreasen N, Hesse C, Davidsson P, et al. Cerebrospinal fluid beta-amyloid(1–42) in Alzheimer disease: differences between early- and late-onset Alzheimer disease and stability during the course of disease. Arch Neurol. 1999;56(6):673–80. https://doi.org/10.1001/archneur.56.6.673.

Authors and Affiliations

Anish Kapadia[1,2] [ORCID] **· Prarthana Desai[3] · Adam Dmytriw[1,2] · Pejman Maralani[1,2] · Chris Heyn[1,2] · Sandra Black[4,5] · Sean Symons[1,2] · For the Alzheimer's Disease Neuroimaging Initiative**

1   Department of Medical Imaging, Sunnybrook Health Sciences Centre, Toronto M4N 3M5, Canada

2   Department of Medical Imaging, University of Toronto, 263 McCaul Street, 4th Floor, Toronto, ON M5T 1W7, Canada

3   Department of Medicine, Maharaja Sayajirao University of Baroda, Vadodra 390002, India

4   Hurvitz Brain Sciences Research Program, Sunnybrook Research Institute, Sunnybrook Health Sciences Centre, University of Toronto, Toronto M4N 3M5, Canada

5   Division of Neurology, Sunnybrook Health Sciences Centre, University of Toronto, Toronto M4N 3M5, Canada